Nonfeedback control of chaos in a microchip solid-state laser by internal frequency resonance

A. Uchida, T. Sato, T. Ogawa, and F. Kannari*
Department of Electrical Engineering, Keio University, 3–14–1 Hiyoshi, Kohoku-ku, Yokohama 223-8522, Japan
(Received 4 May 1998; revised manuscript received 24 July 1998)

Stabilization of a chaotic laser mode to high-period orbits is experimentally and numerically accomplished in a Nd:YVO_4 microchip solid-state laser subject to frequency-shifted optical feedback by applying a pump modulation at well defined conditions. Various periodic orbits, which do not exist in the original chaotic attractor, can be extracted from one chaotic oscillation by varying the pump modulation parameters. Characteristics of the periodic temporal wave form generation can be interpreted by internal frequency resonance among the relaxation oscillation frequencies, the Doppler-shifted frequency of optical feedback, and the pump modulation frequency. [S1063-651X(98)08912-0]

PACS number(s): 05.45.+b, 42.65.Sf

I. INTRODUCTION

Chaos-control techniques have been successfully demonstrated to convert a chaotic motion to a periodic regular motion for emerging attractive applications such as encoded communications [1]. In particular, generation of various periodic orbits from one laser device using chaos control is applicable for pattern-based communications [2], because chaotic attractors contain an infinite number of different periodic orbits. Chaos-control techniques can be classified into two groups: feedback techniques and nonfeedback techniques. Feedback techniques are based on the control method developed by Ott, Grebogi, and Yorke [3] (OGY method), in which chaotic oscillation is stabilized to one of the unstable periodic orbits embedded in a chaotic attractor through the application of a small perturbation to one of the system parameters. In actual systems, an occasional proportional feedback technique [4] and a method using delay coordinates [5] have been demonstrated as improved versions of the OGY methods. Since these feedback techniques require detection of the degree of deviation of the reference unstable periodic state from the chaotic state in real time, the experimental setup for the control must be a closed-loop system [4], and thus tends to be relatively complicated. Moreover, high-speed chaotic oscillations generated in such as laser diodes cannot be stabilized under these feedback techniques.

On the other hand, nonfeedback control techniques [6], in which only a small periodic perturbation is added to the chaotic system and the system converts to a periodic state, have more frequently been used, especially in chaotic laser systems [7–10]. Since this technique requires only small modulation on one of system parameters, a more simple high-speed, open-loop, setup is attainable in experiments. So far, different mechanisms for the nonfeedback control have been proposed: entrainment to goal dynamics [11], parametric excitation of an experimentally adjustable parameter [12], and taming the chaotic system by means of external periodic perturbation [6,13]. However, the basic principle in the nonfeedback technique still remains an open question. Therefore, in spite of the successful application of nonfeedback control schemes, one cannot predict the stabilized state. The conditions for control and the period of the stabilized oscillation strongly depend on the structure of the chaotic attractors and the bifurcation prior to the transition to chaos. In fact, it is not easy to create high-period orbits using the aforementioned nonfeedback techniques, since high-period windows do not exist over a wide range of the bifurcation. Therefore, chaotic oscillations cannot be necessarily stabilized to arbitrarily periodic orbits.

To overcome these issues and predict a regular periodic orbit after control, a goal-oriented scheme [14] has been proposed for a diode resonator. In this scheme one can produce n-periodic orbits by setting the perturbation frequency to $1/n$ times the fundamental oscillation frequency. However, when selecting too large n, the system completely changes. Therefore, there is a limitation on n. Another technique [15] to produce arbitrarily periodic orbits from chaotic attractors has been proposed using the prerecorded time sequence of a chaotic pulsation in chaos-synchronization schemes. However this technique requires the time sequence to be recorded in advance, and the system is very complicated since it requires two synchronized chaotic systems.

In this paper, we propose a nonfeedback chaos-control method that can stabilizes chaotic oscillations into high-period orbits with a certain prediction. Our method is based on an internal frequency resonance among the relaxation oscillation frequencies and the modulation frequencies. We demonstrate our method experimentally and numerically in a laser diode-pumped Nd:YVO_4 microchip solid-state laser. In microchip lasers, chaos in the laser output is generated either by modulation of the intracavity laser power (called loss modulation) or by modulation of the pumping power (pump modulation). A bifurcation in which several periodic orbits exist prior to the transition to chaos is also observed when each of these two modulations is applied to the microchip laser [8,16]. The two different modulation schemes are combined in the same laser oscillator, and a periodic orbit in the bifurcation region in the pump-modulation scheme is mixed with a chaotic attractor produced by the loss-modulation scheme for control of chaos.

II. EXPERIMENTS

Our experimental setup of a laser diode-pumped Nd:YVO_4 microchip solid-state laser is shown in Fig. 1

*FAX: +81 45 563 2773. Electronic address: kannari@elec.keio.ac.jp

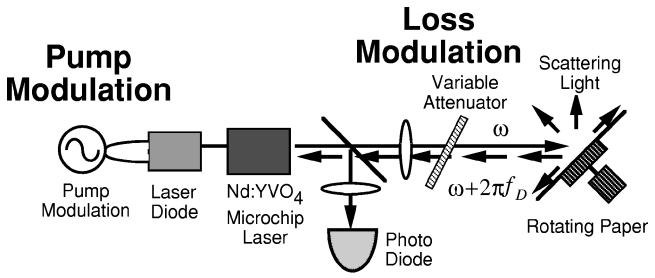

FIG. 1. Schematic of a diode-pumped Nd:YVO_4 microchip laser with frequency-shifted optical feedback (loss modulation) and pump modulation.

[9,10,17]. The microchip laser was an end-pumped 1-mm-long Nd:YVO_4 laser with a Fabry-Perot cavity. An Nd:YVO_4 (NEC) crystal with a Nd concentration of 1.1 at. % was cut along the *a* axis of a crystal. Dielectric cavity mirrors were deposited directly onto the crystal. The output mirror had a reflectivity of 99.0% at 1.064 μm. The opposite mirror had a reflectivity of 99.9% at 1.064 μm, and transmitted the pump at 809 nm. The Nd:YVO_4 chip was bonded to a copper heat sink. A laser diode (Opto Power Corporation OPC-A001-809-FC/100) was used as the pumping source. The output of the laser diode was coupled to a 0.3-m-long optical fiber with 100-μm core diameter, and focused onto the Nd:YVO_4. During our experiments, the output power of the microchip laser was set to a constant of 16 mW at a diode laser current of 580 mA. In this condition, the laser had two longitudinal modes, and the relaxation oscillation frequencies of these two modes were $f_{r1}=1000$ kHz and $f_{r2}=500$ kHz, respectively.

A frequency-shifted feedback light-injection scheme [8–10,17,18] was utilized as a loss-modulation system, as shown in Fig. 1. The laser light is incident upon a rotating circular paper sheet, and weak scattered light whose center frequency is shifted because of the Doppler effect returns to the laser cavity. The laser intensity is then modulated as a result of self-mixing between the two light components in the cavity. At the same time the injection current of the laser diode for pumping is sinusoidally modulated, and this acts as a pump-modulation system. Chaotic instabilities appear in the laser output with only one of the two modulations when the Doppler-shifted feedback light power or the pump-modulation amplitude increases [8,16].

First, we made a bifurcation diagram for the loss-modulation system without pump modulation. The feedback light power was adjusted with a variable optical attenuator. The Doppler-shifted frequency of the feedback light was controlled by the velocity of the rotating paper sheet. When the Doppler-shifted frequency was set to 500 kHz, which was coincident with f_{r2}, bifurcation accompanied by period-1, period-2 and chaotic oscillations was observed as the feedback light power was increased [Fig. 2(a)]. Chaotic oscillations appeared when the transmittance of the variable attenuator was set to greater than 27%. Next, only the pump modulation was applied to the microchip laser without frequency-shifted feedback light. Different types of bifurcation were observed under pump modulation at the modulation frequency $v_c=857$ kHz, as shown in Fig. 2(b). A period-1 regular oscillation shifted to period-6 and period-3 with quasiperiodicity, and finally chaotic oscillations as the

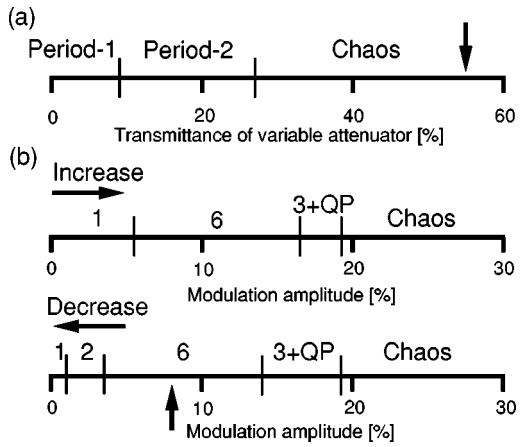

FIG. 2. (a) Bifurcation diagrams of (a) the loss modulation as a function of relative feedback light power and (b) the pump modulation as a function of modulation amplitude. Hysteresis is seen when the direction of the modulation amplitude is changed.

modulation amplitude was increased, whereas the chaotic oscillation changed to period-3 with quasiperiodicity, and period-6, period-2, and period-1 oscillations as the amplitude was decreased. This hysteresis can be seen in the bifurcation diagram. Here the fundamental frequency f_{fun}, which is defined as a frequency of the strongest peak in the power spectrum, of the period-1 and period-2 oscillations, was equal to the pump modulation frequency v_c, whereas f_{fun} of the period-6 and period-3 oscillations was shifted to $\frac{3}{2}v_c$ because the relaxation oscillation frequency f_{r1} located near $\frac{3}{2}v_c$ enhanced the frequency component of $\frac{3}{2}v_c$ as the amplitude of the pump modulation was increased.

Next we combined the loss modulation with the pump modulation in one microchip laser oscillator to stabilize the chaotic oscillation caused by loss modulation [at the condition indicated by an vertical arrow in Fig. 2(a)]. The pump-modulation parameters were selected so that a new periodic orbit was generated without the loss modulation. When the frequency and amplitude of the pump modulation were set to $v_c=857$ kHz and $\Delta w=0.080$, respectively, a periodic laser output in a period-6 orbit was obtained without the loss modulation [corresponding to the vertical arrow in Fig. 2(b)]. Figures 3 and 4 show the temporal wave forms and power spectra of the microchip laser output obtained (a) with only loss modulation, (b) with only pump modulation, and (c) with both modulations. With only the loss modulation [Figs. 3(a) and 4(a)], the temporal wave form of the laser output fluctuates chaotically and the power spectrum spreads. However, when the pump modulation that creates a period-6 orbit [Figs. 3(b) and 4(b)] is applied in addition to the loss modulation, the temporal wave form of the laser output is stabilized to a period-18 regular oscillation, which is different from the periodic orbit caused by the pump modulation, and many discrete narrow peaks appear in the power spectrum [Figs. 3(c) and 4(c)]. Here, the period *n* of the stabilized orbit is determined by the existence of the $1/n$ subharmonics of the fundamental frequency f_{fun} in the power spectrum. These results show that a high-period oscillation whose orbit does not exist in the original chaotic attractor and its bifurcation is obtained.

When the amplitude of the pump modulation is decreased

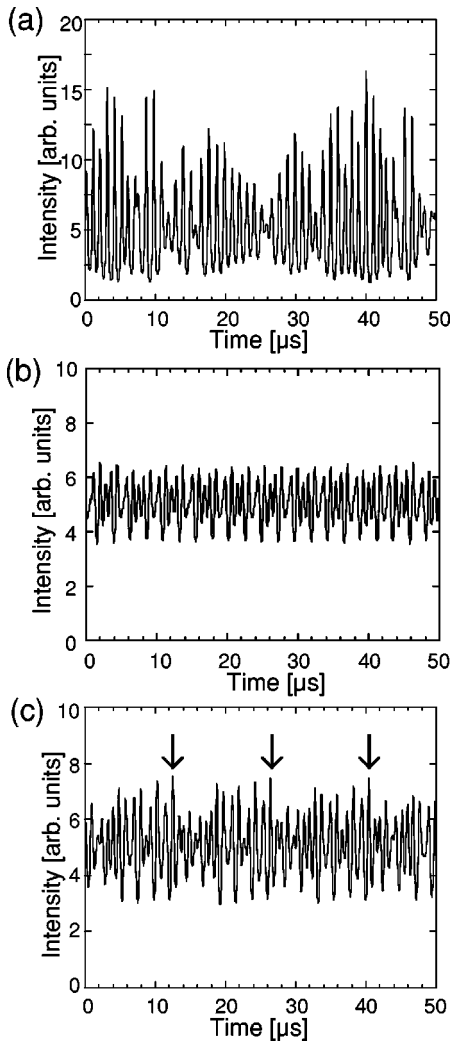

FIG. 3. Temporal wave forms obtained from the experiments: (a) Chaotic oscillation with only loss modulation. (b) Period-6 oscillation with only pump modulation. (c) Period-18 oscillation with loss and pump modulation. Arrows indicate the period.

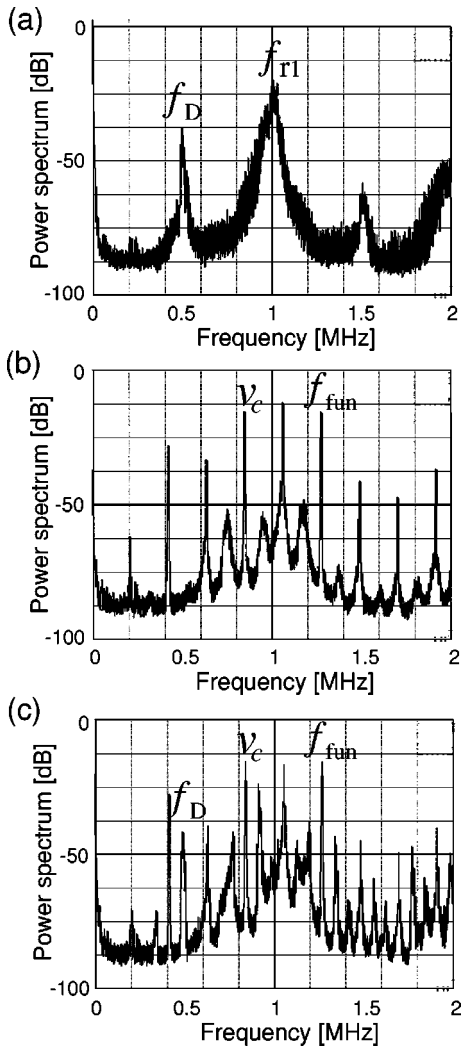

FIG. 4. Power spectra obtained from the experiments: (a)–(c) Same as in Fig. 3. The power spectra are averaged over 20 s.

to 0.035, a period-2 orbit with $f_{\mathrm{fun}}=v_{\mathrm{c}}$ is applied to the chaotic attractor produced by the loss modulation. The laser output is stabilized to a period-12 regular oscillation, which corresponds to the $\frac{1}{12}$ subharmonics of f_{fun}. Therefore, in our control scheme various periodic orbits can be created from a chaotic oscillation by changing the pump-modulation parameters.

We examined the robustness of this stabilization against small variations in the modulation amplitude Δw. With the pump-modulation frequency of 857 kHz, period-12 and period-18 stable oscillation can be maintained in the region of $0.01 \leqslant \Delta w \leqslant 0.06$ and $0.06 \leqslant \Delta w \leqslant 0.16$. These regions are roughly coincident with the regions in which the periodic oscillations exist in Fig. 2(b).

III. NUMERICAL CALCULATIONS AND DISCUSSIONS

To verify our experimental results, we analyzed the chaos-control scheme with a numerical model. The governing equations for multimode solid-state lasers with spatial hole burning were proposed by Tang, Statz, and deMars [19]. In our calculation the scaled Tang-Statz-deMars equations proposed by Otsuka, Chern, and Lih [8] for two-mode lasers were modified as follows:

$$dn_0/dt = w_0[1+\Delta w \cos(2\pi\tau v_{\mathrm{c}} t)] - n_0 - \gamma_1(n_0 - n_1/2)s_1 - \gamma_2(n_0 - n_2/2)s_2, \tag{3.1}$$

$$dn_1/dt = n_0\gamma_1 s_1 - n_1(1+\gamma_1 s_1 + \gamma_2 s_2), \tag{3.2}$$

$$dn_2/dt = n_0\gamma_2 s_2 - n_2(1+\gamma_1 s_1 + \gamma_2 s_2), \tag{3.3}$$

$$ds_1/dt = K[\gamma_1(n_0 - n_1/2) - 1]s_1 + s_1 Km \cos(2\pi\tau f_D t), \tag{3.4}$$

$$ds_2/dt = K[\gamma_2(n_0 - n_2/2) - 1]s_2 + s_2 Km \cos(2\pi\tau f_D t), \tag{3.5}$$

where n_0 is the spatially averaged population inversion density with spatial hole burning normalized by the threshold value, $n_{1,2}$ is the first order Fourier component of population inversion density for the two modes, $s_{1,2}$ is the photon density normalized by the steady-state value for the two modes, $\gamma_{1,2}$ is the gain ratio to the first lasing mode, and the subscripts 1 and 2 show a corresponding mode. $K=\tau/\tau_p$ is a

ratio of the lifetime, where τ is the population lifetime of Nd:YVO_4 and τ_p is the photon lifetime in the laser cavity. m is the ratio of the feedback light amplitude to the radiation amplitude. f_D is the Doppler-shifted frequency of the feedback light field. m and f_D correspond to the amplitude and frequency of the loss modulation, respectively. Time is scaled by τ. w_0 is the bias component of the scaled pump power. Here the temporal variation of the phase difference between the lasing field and the feedback light field can be neglected because of relatively weak feedback light [9]. The first right-hand term of Eq. (3.1) and the second right-hand terms of Eqs. (3.4) and (3.5) correspond to the effect of the pump modulation and loss modulation, respectively.

The K parameter for our microchip laser is relatively high at 7.67×10^4 causing high sensitivity against weak external light injection, since τ and τ_p are 88 μs and 1.15 ns, respectively. When we set $w_0=5.2$, $\gamma_1=1$, and $\gamma_2=0.875$, the relaxation oscillation frequencies for two longitudinal modes were $f_{r1}=1000$ kHz and $f_{r2}=500$ kHz, which were the same values as those observed in our experiments. When we set a Doppler-shifted frequency $f_D=500$ kHz and a feedback ratio $m=0.0025$, chaotic instabilities appeared in the laser output.

When the pumping was modulated with a frequency of $v_c=857$ kHz and an amplitude of $\Delta w=0.08$, a period-6 signal was generated without the loss modulation, and this period-6 orbit was utilized to suppress the chaotic oscillations caused by the loss modulation. Figures 5 and 6 show the temporal wave forms and the power spectra of the microchip laser output obtained by use of numerical calculations (a) with only loss modulation (chaos), (b) with only pump modulation (period 6) and (c) with both of the two modulations (period 18). The chaotic oscillation is stabilized to a period-18 regular oscillation by mixing a new period-6 orbit and the chaotic attractor. The discrete spectrum components are clearly observed at regular intervals of $\frac{1}{18}f_{\mathrm{fun}}$. These results agree well with our experimental results shown in Fig. 3 and 4.

The mechanism of the stabilization to the period-18 oscillation can be explained by internal frequency resonance [20] among the relaxation oscillation frequencies f_{r1} and f_{r2} and the modulation frequencies f_D and v_c (f_{fun}). When only the pump modulation is applied to a microchip laser which has two commensurable relaxation oscillation frequencies (e.g., $f_{r1}=2f_{r2}$), strong internal resonance occurs [20] and a period-6 orbit is obtained, where there is a series of subharmonic peaks at regular intervals of $\frac{1}{6}f_{\mathrm{fun}}$ in the power spectrum, as shown in Fig. 6(b). When both the pump modulation and loss modulation are simultaneously applied to the microchip laser, the internal resonance leads to stable frequency mixing between f_D and one of the subharmonics of f_{fun} (the nearest frequency component to f_D, in this case $\frac{1}{3}f_{\mathrm{fun}}$), and thus resonantly create a new subharmonic whose frequency is shifted upwards from f_D by $\frac{1}{18}f_{\mathrm{fun}}=f_D-\frac{1}{3}f_{\mathrm{fun}}$. Then f_D and this new subharmonic create another higher subharmonic. These processes occur simultaneously, and f_D and subharmonics of f_{fun} resonantly create a series of subharmonics with regular intervals of $\frac{1}{18}f_{\mathrm{fun}}$ from the broad spectrum [Fig. 6(c)]. A condition for stable periodic oscillations is that the ratio of f_{fun} and f_D is set to a rational number. In this case, these subharmonics are locked to each other [21],

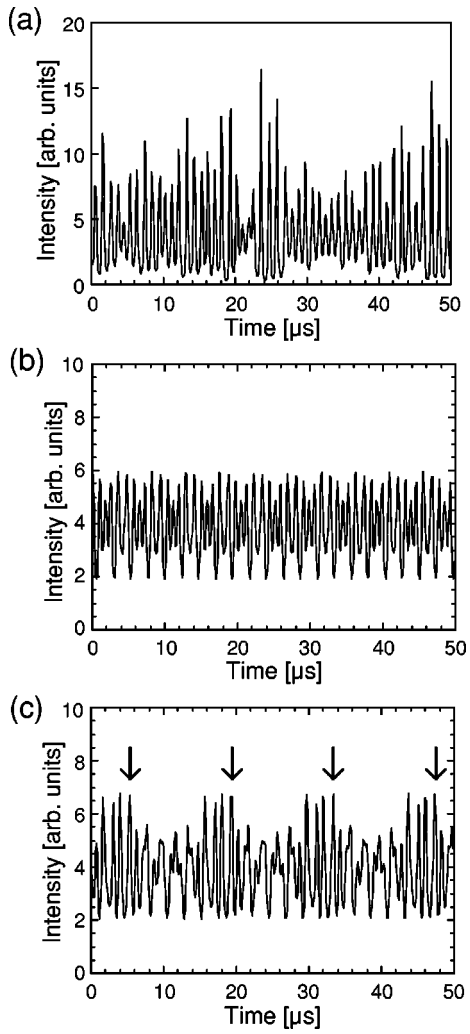

FIG. 5. Temporal wave forms obtained from the numerical calculations: (a)–(c) same as in Fig. 3.

and the stability of the periodic oscillation is maintained even at high-period orbits. Through this resonant frequency mixing and frequency locking, chaotic oscillation is suppressed and a new stable period-18 oscillation is generated.

Now a question arises as to what condition is required to accomplish to control chaos. To answer this question, we compared the bifurcation diagram of pump modulation with that obtained with both pump and loss modulation as the amplitude of the pump modulation Δw was decreased (Fig. 7). The frequency of the pump modulation v_c was set to 857 kHz, and the parameters of the loss modulation was set to $f_D=500$ kHz and $m=0.0025$, respectively. With only pump modulation, the chaotic oscillation changes to period 3 with quasiperiodicity, and period-6, period-2, and period-1 oscillations as Δw is decreased [Fig. 7(a)], which is coincident with our experimental results shown in Fig. 2(b). When the pump modulation is applied to a chaotic oscillation generated by the loss modulation, stabilized periodic oscillations appear, as shown in Fig. 7(b). In the region of $0.015\leqslant\Delta w\leqslant 0.09$, the stabilized oscillations exhibiting period 24 consist of two coexistent period-12 orbits with the phase difference of π. The region of $0.015\leqslant\Delta w\leqslant 0.09$, in which the periodic oscillation exists in Fig. 7(b), is roughly coincident with the region of $0.015\leqslant\Delta w\leqslant 0.13$ in which

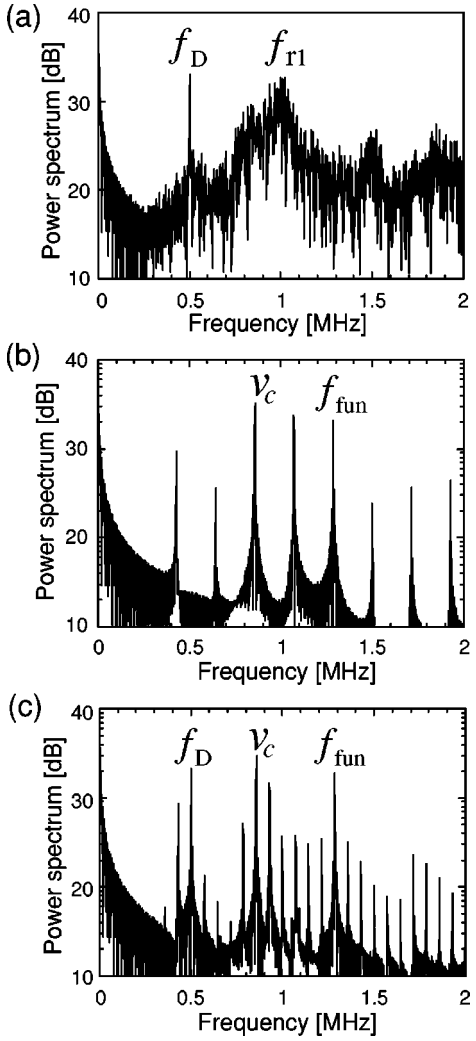

FIG. 6. Power spectra obtained from the numerical calculations: (a)–(c) same as in Fig. 3. The power spectra are averaged over 20 s.

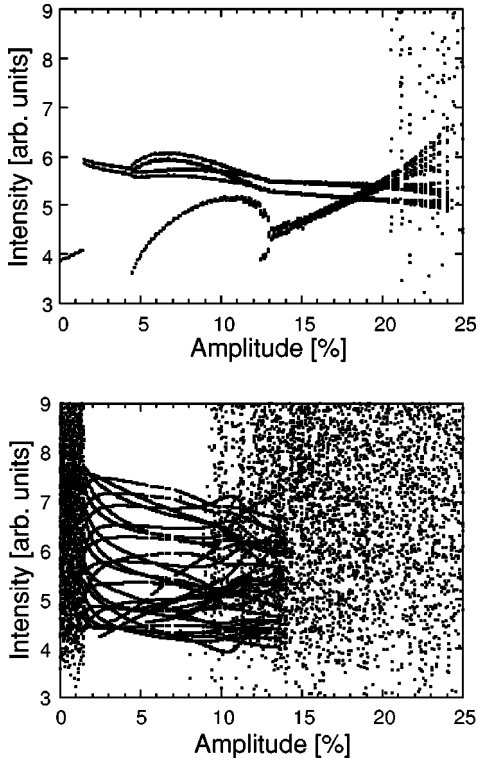

FIG. 7. Bifurcation diagrams as a function of the amplitude of the pump modulation (a) with only pump modulation, and (b) with loss and pump modulation.

the periodic orbits exist in Fig. 7(a). In higher pump modulations of $\Delta w > 0.09$, the dynamics of the entire system are changed due to a mutual strong coupling of two modulation systems, and chaos control cannot be achieved. From these results, we can conclude that the selection of the pump-modulation parameters for generation of a periodic orbit is very important to control chaos in the wide range of Δw except for much larger Δw.

To generate arbitrary periods of the stabilized orbits from chaos, we need to set two parameters: the period of a periodic orbit caused by the pump modulation and the ratio between the two modulation frequencies f_D and v_c. The period in a stabilized oscillation depends on these two parameters. Actually, v_c has to be set at a certain value to resonate with the relaxation oscillation frequencies to create a period-k orbit. The period-k orbit always forms discrete subharmonic peaks at regular intervals of $(1/k)f_{\mathrm{fun}}$ in the spectrum. When the ratio between f_D and $f_{\mathrm{fun}}(=\frac{3}{2}v_c)$ is set to $m{:}n(n$ is a multiple of $k)$, many discrete spectral peaks appear at constant intervals of $(1/n)f_{\mathrm{fun}}$ in the spectrum because of resonant frequency mixing. Consequently, a period-n temporal wave form, which is a multiple of period k, can be generated. In our results, the period-18 temporal wave form was formed by the selection of $k=6$, $m=7$, and $n=18$.

According to this principle, only certain frequencies of the pump modulation v_c and frequencies very close to these $[v_c \pm 3$ kHz$]$ are allowed as the stabilized periodic oscillations, since stabilized periodic oscillations can be obtained only when the ratio of the frequencies between the loss and pump modulation is just or close to a rational number. Figures 8(a) and (b) show the power spectra of the period-21 $(m{:}n=8{:}21)$ and period-24 $(9{:}24)$ oscillations which can be generated at different frequencies of the pump modulation with $v_c=875$ and 889 kHz, respectively. There are discrete spectrum components at regular intervals of $\frac{1}{21}f_{\mathrm{fun}}$ and $\frac{1}{24}f_{\mathrm{fun}}$ in Figs. 8(a) and 8(b), respectively. In these cases, a period-3 orbit created by the pump modulation is mixed with a chaotic attractor for controlling chaos. Even higher-period orbits such as periods 27, 30, and 33 can be generated as we predict by increasing v_c until the periodic orbit cannot be created over the periodic region in the bifurcation.

When irrational ratios are selected for the loss- and pump-modulation frequencies, chaotic oscillations are stabilized to quasiperiodic orbits because frequency locking between f_D and subharmonics of f_{fun} cannot be achieved. For example, there are discrete spectrum components at irregular intervals as shown in Fig. 8(c) with $v_c=865$ kHz. Therefore, we can assign periods of the stabilized orbits only when setting the two modulation frequencies to a certain rational value.

Next we investigate the conditions for control when the amplitude of the loss modulation, m, is varied. Figure 9 shows bifurcation diagrams plotted against m (a) with only loss modulation and (b) with loss and pump modulation. With only loss modulation, a period-1 oscillation is changed to period-2, quasiperiodic and chaotic oscillations in lower

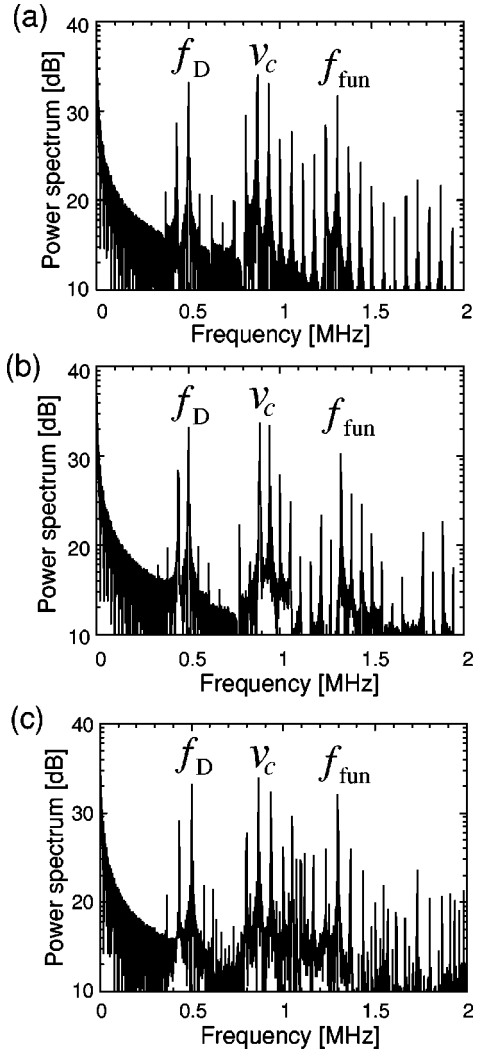

FIG. 8. Power spectra with different periods (a) Period 21 (v_c = 875 kHz), (b) Period 24 (v_c = 889 kHz). (c) Quasiperiodicity (v_c = 865 kHz).

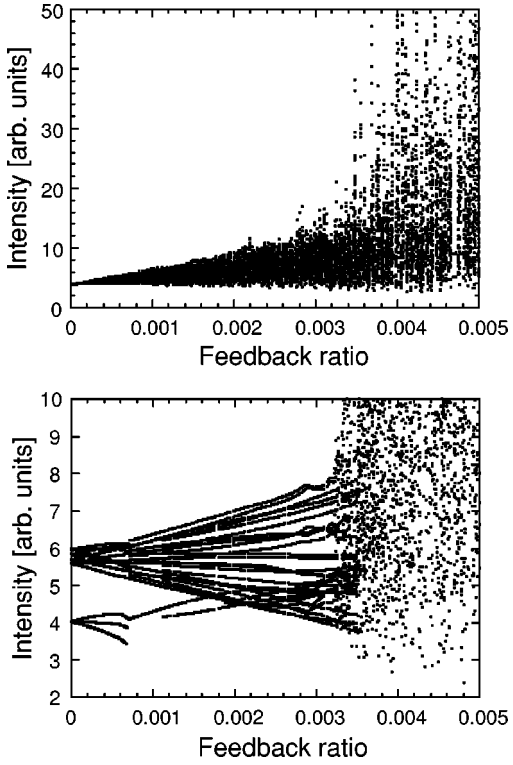

FIG. 9. Bifurcation diagrams as a function of the amplitude of the loss modulation (a) with only loss modulation, and (b) with loss and pump modulation.

regions of m in Fig. 9(a) as the feedback light power is increased. When the frequency and amplitude of the pump modulation are set to 857 kHz and 0.05, respectively, and the pump modulation with a period-6 orbit is applied, two coexistent period-12 oscillations are generated in the region of $0.0011 \leqslant m \leqslant 0.0032$, as shown in Fig. 9(b). The lower limit $m = 0.0011$ roughly corresponds to the limit at which the dynamics changes from quasiperiodic to chaotic oscillations in the loss modulation. Chaotic oscillations cannot be stabilized at $m > 0.0032$ where the shape of chaotic oscillations changes to a pulselike behavior with high peak intensity (chaotic spiking oscillation) from the continuous wave-like behavior, such as shown in Fig. 5(a). Therefore, our control scheme is applicable at the small amplitude of the loss modulation, where the entire chaotic dynamics do not change.

Our scheme is essentially different from conventional nonfeedback chaos-control methods, which apply a small perturbation to one of the system parameters. To suppress chaos, we need to use a new periodic orbit that already exists in a bifurcation region caused by the pump modulation. Since the pump-modulation amplitude needs to be large enough to generate a periodic orbit in the bifurcation, as shown in Fig. 2(b), the modulation amplitude in our scheme is larger than typical perturbations used in conventional chaos-control techniques. Thus the structure of the original chaotic system is changed by applying the pump modulation. A new orbit is created from the internal resonance between the loss- and pump-modulation frequencies, and the chaos is stabilized to this new orbit. Therefore, various periodic orbits, which are not restricted to those in the original chaotic attractor, can be generated as a result of chaos stabilization. Even high-period orbits that are not realized by using conventional nonfeedback chaos-control techniques are obtainable.

IV. CONCLUSIONS

We propose a nonfeedback chaos-control scheme, where various high-period oscillation states with different periods are available as stabilized modes, even if these states do not exist in the original chaotic attractor. Suppression of chaotic oscillation is achieved by internal frequency resonance among the relaxation oscillation frequencies and the modulation frequencies. The period of stabilized oscillations can be established by selection of a ratio of the two modulation frequencies. Our hybrid chaotic system can create a variety of periodic orbits, and could be useful as an arbitrary temporal wave form generator in optical information processing and optical communications.

ACKNOWLEDGMENTS

We gratefully acknowledge Professor P. Mandel, Universite Libre de Bruxelles, and Professor K. Otsuka, Tokai University, for helpful discussions.

[1] K. M. Kuomo and A. V. Oppenheim, Phys. Rev. Lett. **71**, 65 (1993).
[2] F.-J. Kao and J.-L. Chern, LEOS Newsletter **10**, 16 (1996).
[3] E. Ott, C. Grebogi, and J. A. Yorke, Phys. Rev. Lett. **64**, 1196 (1990).
[4] E. R. Hunt, Phys. Rev. Lett. **67**, 1953 (1991); R. Roy, T. W. Murphy, Jr., T. D. Maier, Z. Gills, and E. R. Hunt, *ibid.* **68**, 1259 (1992); P. Colet, R. Roy, and K. Wiesenfeld, Phys. Rev. E **50**, 3453 (1994).
[5] K. Pyragas, Phys. Lett. A **170**, 421 (1992); S. Bielawski, D. Drezoier, and P. Glorieux, Phys. Rev. E **49**, R971 (1994).
[6] Y. Braiman and I. Goldhirsch, Phys. Rev. Lett. **66**, 2545 (1991).
[7] R. Meucci, W. Gadomski, M. Ciofini, and F. T. Arecchi, Phys. Rev. E **49**, R2528 (1994); A. T. Ryan, G. P. Agrawal, G. R. Gray, and E. C. Gage, IEEE J. Quantum Electron. **QE-30**, 668 (1994); Y. Liu, N. Kikuchi, and J. Ohtsubo, Phys. Rev. E **51**, R2697 (1995); M. Ciofini, R. Meucci, and F. T. Arecchi, *ibid.* **52**, 94 (1995); T. Tsukamoto, M. Tachikawa, T. Sugawara, and T. Shimizu, Phys. Rev. A **52**, 1561 (1995); P. Colet and Y. Braiman, Phys. Rev. E **53**, 200 (1996); N. Watanabe and K. Karaki, Opt. Lett. **21**, 1256 (1996); A. N. Pisarchik, V. N. Chizhevsky, R. Corbalan, and R. Vilaseca, Phys. Rev. E **55**, 2455 (1997); R. Dykstra, A. Rayner, D. Y. Tang, and N. R. Heckenberg, *ibid.* **57**, 397 (1998).
[8] K. Otsuka, J.-L. Chern, and J.-S. Lih, Opt. Lett. **22**, 292 (1997).
[9] A. Uchida, T. Sato, M. Takeoka, and F. Kannari, Jpn. J. Appl. Phys. **36**, L912 (1997).
[10] A. Uchida, T. Sato, and F. Kannari, Opt. Lett. **23**, 460 (1998).
[11] J. L. Breeden, F. Dinkelacker, and A. W. Hübler, Phys. Rev. A **42**, 5827 (1990); E. A. Jackson, Physica D **50**, 341 (1991); R. Mettin, A. Hübler, A. Scheeline, and W. Lauterborn, Phys. Rev. E **51**, 4065 (1995).
[12] R. Lima and M. Pettini, Phys. Rev. A **41**, 726 (1990); L. Fronzoni, M. Giocondo, and M. Pettini, *ibid.* **43**, 6483 (1991); Y. Kivshar, F. Rodelsperger, and H. Benner, Phys. Rev. E **49**, 319 (1994).
[13] R. Chacon, Phys. Rev. E **50**, 750 (1994); Z. Qu, G. Hu, G. Yang, and G. Qin, Phys. Rev. Lett. **74**, 1736 (1995).
[14] H.-J. Li and J.-L. Chern, Phys. Rev. E **54**, 2118 (1996).
[15] K. Pyragas, Phys. Lett. A **181**, 203 (1993); A. Kittel, K. Pyragas, and R. Richter, Phys. Rev. E **50**, 262 (1994); T. Tsukamoto, M. Tachikawa, T. Tohei, T. Hirano, T. Kuga, and T. Shimizu, *ibid.* **56**, 6564 (1997).
[16] P. Mandel, M. Georgiou, K. Otsuka, and D. Pieroux, Opt. Commun. **100**, 341 (1993).
[17] S. Okamoto, H. Takeda, and F. Kannari, Rev. Sci. Instrum. **66**, 3116 (1995).
[18] K. Otsuka, J. Appl. Phys. **31**, L1546 (1992).
[19] C. L. Tang, H. Statz, and G. deMars, J. Appl. Phys. **34**, 2289 (1963).
[20] D. Pieroux, T. Erneux, and P. Mandel, Phys. Rev. A **54**, 3409 (1996).
[21] K. Otsuka, D. Pieroux, J.-Y. Wang, and P. Mandel, Opt. Lett. **22**, 516 (1997).